JOURNAL OF GEOPHYSICAL RESEARCH, VOL. 112, D23106, doi:10.1029/2006JD008303, 2007

Water and energy budgets of hurricanes: Case studies of Ivan and Katrina

Kevin E. Trenberth,[1] Christopher A. Davis,[1] and John Fasullo[1]

Received 1 December 2006; revised 27 August 2007; accepted 12 September 2007; published 12 December 2007.

[1] To explore the role of hurricanes in the climate system, a detailed analysis is made of the bulk atmospheric moisture budget of Ivan in September 2004 and Katrina in August 2005 from simulations with the Weather and Research Forecasting (WRF) model at 4 km resolution without parameterized convection. Heavy precipitation exceeding 20 mm h^{-1} in the storms greatly exceeds the surface flux of moisture through evaporation, and vertically integrated convergence of moisture in the lowest 1 km of the atmosphere from distances up to 1600 km is the dominant term in the moisture budget, highlighting the importance of the larger-scale environment. Simulations are also run for the Katrina case with sea surface temperatures (SSTs) increased by +1°C and decreased by −1°C as sensitivity studies. For hours 42 to 54 after the start of the simulation, maximum surface winds increased about 4.5 m s^{-1} (9%), and sea level pressure fell 11.5 hPa per 1°C increase in tropical SSTs. Overall, the hurricane expands in size as SSTs increase, the environmental atmospheric moisture increases at close to the Clausius-Clapeyron equation value of about 6% K^{-1} and the surface moisture flux also increases mainly from Clausius-Clapeyron effects and the changes in intensity of the storm. The environmental changes related to human influences on climate since 1970 have increased SSTs and water vapor, and the results suggest how this may have altered hurricanes and increased associated storm rainfalls, with the latter quantified to date to be of order 6 to 8%.

Citation: Trenberth, K. E., C. A. Davis, and J. Fasullo (2007), Water and energy budgets of hurricanes: Case studies of Ivan and Katrina, *J. Geophys. Res.*, *112*, D23106, doi:10.1029/2006JD008303.

1. Introduction

[2] What role, if any, do hurricanes and tropical storms have in our climate system? Or, alternatively, how do hurricanes relate to the large-scale environment? These rather fundamental questions are the motivation for the research outlined here. The main fuel for hurricanes is the latent heat release in convection acting collectively and organized by the hurricane circulation to drive the storm [e.g., *Krishnamurti et al.*, 2005; *Braun*, 2006]. Hence the perspective put forward here is from the water cycle and the latent energy that arises from condensation of moisture in precipitation, while the moisture in turn comes from evaporation from the ocean surface, in part brought about by the storm itself. In particular, the bulk water budgets for some simulated hurricanes are assessed and the three key components we focus on are the surface moisture or, equivalently, latent energy flux into the atmosphere, the convergence of atmospheric moisture into the storm through atmospheric wind transport, and the precipitation. Energy aspects are the focus of a companion paper [*Trenberth and Fasullo*, 2007]. Changes in precipitation and associated flooding over land are also of considerable interest from a societal standpoint.

[3] Early estimates of the water and energy budgets in hurricanes were provided by *Palmén and Riehl* [1957] and *Malkus and Riehl* [1960], and for individual storms by *Riehl and Malkus* [1961] and *Miller* [1962]. This work was nicely summarized by *Palmén and Newton* [1969] and suggested the dominance of the inflow of latent heat energy in the form of moisture for the tropical cyclones, with efficiencies of kinetic energy production of only 3%. For cylinders 1° latitude radius from the center of the storm, the case studies suggested 3×10^{14} W latent heat inflow contributions versus 0.3 to 0.6×10^{14} W for the surface flux. For a 2° radius, *Palmén and Riehl* [1957] found 5.5×10^{14} W inflow of latent heat and suggested the total energy export of the storm was 8.8×10^{14} W. *Anthes* [1974] discussed the energetics of tropical cyclones as well as the water vapor budget and showed from a simple analytic model how the horizontal transport of water vapor toward the hurricane center across various radii compared to evaporation inside that radius. He also summarized empirical studies that showed the dominance of transport over evaporation in several storms for radii of 111 km and 150 km. *Kurihara* [1975] examined water budgets for an axisymmetric simulated hurricane and found out to 500 km radius that

[1]National Center for Atmospheric Research, Boulder, Colorado, USA.

0148-0227/07/2006JD008303$09.00

evaporation from the surface was about 20% of the rainfall and 25% of the transport of moisture into the storm, but the evaporation contribution was very small in the inner core region, although vital for the storm to exist, as it raised equivalent potential temperature enough to allow the hurricane to develop.

[4] A comprehensive summary of the understanding of hurricanes and their relationship to climate is given by *Emanuel* [2003] and it provides an excellent basis for the perspective put forward here, however, it lacked a discussion of precipitation and the water cycle, which we consider relevant for understanding climate change influences on tropical storms. With new satellite instrumentation, much has been learned about precipitation and its structure from the Tropical Rainfall Measurement Mission (TRMM). The most definitive climatology of rainfall in hurricanes comes from TRMM estimates [*Lonfat et al.*, 2004]. They show that average rain rates are 11 to 13 mm h^{-1} from the eye to 50 km radius for category 3–5 hurricanes, dropping to 7 and 3 mm h^{-1} at 100 and 180 km radii. On average for category 1–2 hurricanes the peak values are 6 to 7 mm h^{-1}.

[5] The most detailed study of the water budget in a hurricane is for Bonnie in 1998 by *Braun* [2006], who also provides a nice review of past work and discusses approximations and issues from previous work. In the numerical simulation Braun finds that 15 to 20% of the precipitation in the hurricane comes from artificial moisture sources associated with setting numerically derived negative mixing ratios to zero. He confirms that surface fluxes of moisture into the storm are only a small fraction of the water vapor transported inward in the boundary layer. A central purpose of this paper is to also provide estimates of water budget terms for tropical storms and this will in turn have implications for how hurricanes interact with and depend on their environment.

[6] As observations of surface fluxes are lacking, the approach used here is to analyze results of some case studies with the high-resolution (4 km) Weather and Research Forecasting (WRF) model simulations for actual observed hurricanes in 2004 (mainly Ivan) and 2005 (mainly Katrina). However, these model runs are not initialized other than with a global-scale analysis. The forecast tracks are very good, but the model spins up from a weaker than observed initial vortex for at least the first 12 h and its evolution in intensity does not match the observations. Also, sea surface temperatures (SSTs) are specified as observed, and thus do not change as the storm develops. Therefore these are regarded as possible storms in a realistic environment, although not replications of the observed storms. As the moisture budgets computed are robust from run to run and storm to storm, the main results are not sensitive to details. We have also run the Katrina case with perturbations in SSTs of ±1°C to perform sensitivity tests and check ideas on how surface fluxes and precipitation change with the environmental variables.

[7] In the following section we first review the background state of knowledge on both the energetics and water cycle of storms and tropical storms and put forward a basic theory for interpreting the model results. Section 3 summarizes the case studies with WRF, including those with altered SSTs. Section 4 discusses the results and draws conclusions related to climate change.

2. Storm Energetics and Water Cycle

[8] An overall view of the flow of energy through the climate system is given by *Trenberth and Stepaniak* [2003a, 2003b, 2004]. Tropical cyclones are driven by enthalpy fluxes from the sea, mainly in the form of evaporation of moisture, and are limited mostly by surface drag [*Bister and Emanuel*, 1998]. Air at the surface air spirals into the center of the storm in contact with the ocean and picks up moisture from the surface. Further, tropical cyclones create a cold wake owing to the cooling of the ocean and mixing the upper ocean [*Emanuel*, 2001, 2003]. A detailed analysis by *Walker et al.* [2005] of the cold wake left behind hurricane Ivan in 2004 reveals SST cooling of 3–7°C in two areas along Ivan's track, related closely to the depth of the mixed layer and upper ocean heat content. Energy considerations are covered in detail by *Trenberth and Fasullo* [2007].

[9] Water vapor plays a major role in climate not only as a dominant feedback variable in association with radiative effects but also in the moist dynamics in weather systems. In the lower troposphere, water vapor in the atmosphere acts as the main resource for precipitation in all weather systems, providing latent heating in the process and dominating the structure of diabatic heating in the troposphere [*Trenberth and Stepaniak*, 2003a, 2003b]. The amount of total column water vapor in the atmosphere depends on temperature and ranges up to about 55 mm in the tropics, with a global mean of about 25 mm [*Trenberth and Guillemot*, 1998; *Trenberth and Smith*, 2005]. Observations of column-integrated water vapor (precipitable water) based on the SSM/I data over the oceans [*Trenberth et al.*, 2005] reveal linear upward trends from 1988 to 2003 for the global oceans of 0.40 ± 0.09 mm $decade^{-1}$ or about 1.3% $decade^{-1}$. Most of the patterns associated with the interannual variability and linear trends can be reproduced by scaling the observed SST changes by 7.8% K^{-1}, which is consistent with a constant relative humidity or, in other words, changes from the Clausius-Clapeyron equation of about 7% K^{-1} (globally), with the difference due to use of SST versus air temperature.

[10] *Trenberth* [1999] estimates that for extratropical cyclones, on average about 70% of the precipitation comes from moisture that was already in the atmosphere at the time the storm formed, while the rest comes from surface evaporation, or more generally evapotranspiration, during the course of the storm's evolution. For thunderstorms, owing to their short lifetime, virtually all of the moisture that is precipitated out comes from water vapor resident in the atmosphere at the time the storm forms. Average evaporation rates are typically 0 to 6 mm d^{-1}, with a global mean of 2.8 mm d^{-1} [*Kiehl and Trenberth*, 1997; *Trenberth and Guillemot*, 1998]. However, precipitation is intermittent and most of the time does not occur. Globally *Trenberth et al.* [2003] suggest that because precipitation areas cover perhaps about 1/16th of the globe, the average precipitation rate is 16 times the average evaporation rate. While this obviously depends on the threshold for measurable precipitation and varies greatly temporally and spatially, especially with latitude, the exact value is not critical to the arguments

here. However, it means that on average, the storm-scale circulation reaches out about factor of 3 to 5 times the radius of the precipitating area to gather the available moisture in the atmosphere. These numbers arise simply from the observed precipitation rates versus the known moisture in the atmosphere, and recognition that perhaps only 30% of that moisture is available (i.e., the relative humidity can be reduced from 100% to 70%, but not to 0%, over broad regions) [*Trenberth et al.*, 2003].

[11] The key point is that there is typically a huge mismatch between evaporation rates and precipitation rates in storms except where precipitation is light. One exception is rapid cyclogenesis off the East Coast of the United States where surface latent heat fluxes have been noted to exceed 1500 W m^{-2} for very short times [e.g., *Nieman and Shapiro*, 1993], equivalent to order 50 mm d^{-1} evaporation (but typically occurring for only a few hours). Even hurricanes, where evaporation from high SSTs above about 26°C helps fuel the storm along with large-scale moisture convergence as it spirals into the storm [e.g., *Krishnamurti et al.*, 2005] as part of a larger-scale overturning circulation, also seem to fit this pattern [*Braun*, 2006]. The relative proportion of local evaporation versus moisture transport into hurricanes is evaluated below for some case studies. We are unaware of reliable estimates of evaporation in hurricanes, and published measurements do not exist in winds above about 20 m s^{-1} although some progress has been made in the Coupled Boundary Layer Air-Sea Transfer Experiment (CBLAST) [*Black et al.*, 2007; *Chen et al.*, 2007], and explored for the WRF model we use by *Davis et al.* [2007]. Instead, as in the work by *Braun* [2006], we can evaluate the surface fluxes of moisture in state-of-the-art hurricane model simulations and forecasts and assess the relative contributions in the model framework.

[12] Although limited globally by the available surface energy, evaporation and thus latent energy into the atmosphere can increase locally in a transient fashion with a storm. The simplified bulk flux formula gives the evaporation as

$$E = \rho_a C_L V(q_s(T_s) - q(T)) = \rho_a C_L V q_s(T_s)(1 - RH^*) \qquad (1)$$

where C_L is the exchange coefficient, ρ_a is the air density, q is the specific humidity at temperature T or T_s = SST, q_s is the saturation value of q, RH is the relative humidity, and V is the wind speed. Here $RH^* = RH\, q_s(T)/q_s(T_s)$. Because the relative humidity is observed to not change much, the term RH* may not vary much and a dominant dependency for E is the saturation specific humidity at the SST, which is governed by Clausius-Clapeyron, and the wind speed V. Hence for transient changes, a component of E is likely to go up at about the same rate as observed in the atmosphere for the change in storage, or about 6% K^{-1} rise in atmospheric temperature in the tropics. Further complications arise from possible intensification of the storm, and thus increases in wind speed and surface fluxes. Objectively analyzed latent heat fluxes from 1981 to 2005 reveal increases of about 10% that are consistent with Clausius-Clapeyron effects and increases in SSTs [*Lu and Weller*, 2007].

[13] Moisture in the atmosphere is observed to be enhanced by about 6% (surface tropics) to 7% (lower troposphere, global) per K change in atmospheric temperature [*Trenberth*, 1998; *Trenberth et al.*, 2003]. Further, enhanced moisture may be converted to precipitation at the same enhanced rate, given the same boundary layer mass convergence. However, then the extra latent heat has to be compensated for by adiabatic cooling as the air rises (i.e., in the thermodynamic equation diabatic heating is offset mainly by the term ωS, where S is static stability). Thus it is reasonable to assume that the both the radial wind v_r and q should increase by 6%, thereby increasing the moisture flux $v_r q$ by 12% (coming from 1.06^2). The basis for this assumption is the Eliassen balanced model [*Eliassen*, 1951] which includes a linear differential relation between the transverse circulation strength (here represented by v_r) and the diabatic heating. The diabatic heating will increase proportionately to q and hence so will v_r. This would correspond to the expected increase in rainfall rates in the storm. On the basis of *Trenberth et al.* [2005], the increase in the tropics would be about 14% K^{-1} increase in SST (since the atmospheric temperature increase tends to be larger than the SST increase). The main complications with this simple argument come from possible changes in the static stability and where the latent heat is realized relative to the eye of the storm, as discussed later. We will test these theoretical ideas in the numerical experiments that follow.

3. Case Studies Using WRF

[14] The WRF model [*Michalakes et al.*, 2001], specifically the Advanced Research WRF (hereafter referred to simply as WRF [*Skamarock et al.*, 2005; *Davis et al.*, 2007]) has been used in real time to forecast several hurricanes during 2004 and 2005. It features 34 levels in the vertical with high resolution in the boundary layer. It operates on a 450 × 500 4-km grid (1800 by 2000 km). The model has a terrain-following hydrostatic pressure vertical coordinate, uses third-order Runge-Kutta spilt-explicit time differencing and fifth-order upwind or sixth-order differencing for advection to compute numerics accurately. It conserves mass, momentum, entropy, and scalars using flux form prognostic equations. This version of WRF avoids the use of a cumulus parameterization by using the 4-km grid and treating deep convection and precipitation formation explicitly using a simple cloud scheme in which cloud water, rain and snow were predicted variables. We consider this a major advantage over the parameterized convection model results of *Knutson and Tuleya* [2004]. Results with more sophisticated schemes in WRF show similar results concerning fluxes and precipitation. The surface layer formulation utilizes the bulk aerodynamic formulations in which the drag and enthalpy coefficients are a specified function of surface wind speed [*Charnock*, 1955]. Sensitivity tests of the model to changes in the surface flux formulation have been reported by *Davis et al.* [2007] although proper wind speed dependence on exchange coefficients remains a topic of active research [e.g., *Black et al.*, 2007; *Chen et al.*, 2007]. The boundary layer scheme is a first-order closure scheme, meaning that turbulence is diagnosed entirely in terms of grid-scale variables [*Noh et al.*, 2003].

[15] The WRF simulations were initialized from the Global Forecast System (GFS) on a 1° × 1° grid from the

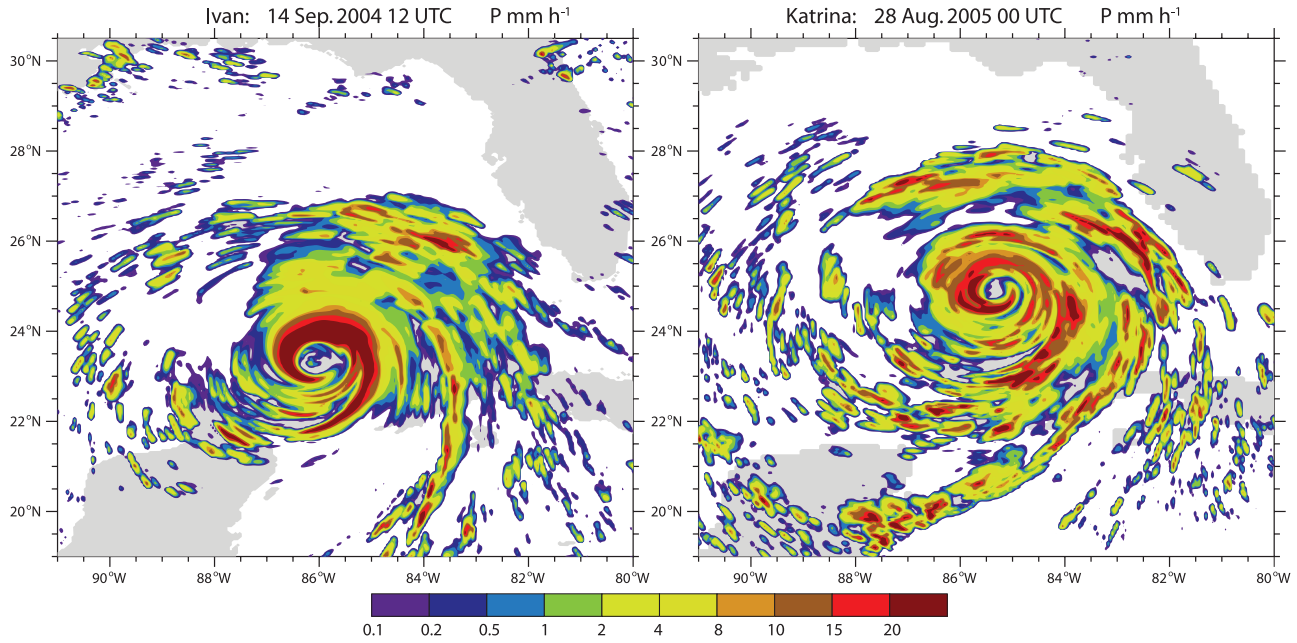

Figure 1. Precipitation (mm h^{-1}) fields for simulated hurricanes (left) Ivan at 1200 UTC 14 September 2004 and (right) Katrina at 0000 UTC 28 August 2005.

National Centers for Environmental Prediction (NCEP). However, WRF was able to spin up a highly realistic structure in about 12 h and sample structures in the center of the periods investigated in more detail below are given for Ivan and Katrina in Figure 1. In many cases the forecasts of track and intensity have been excellent for more than 48 h in advance. Nevertheless, intensity is difficult to simulate correctly for a number of reasons related especially to initialization, feedbacks (e.g., from ocean and SST changes) and inner core dynamics [*Emanuel*, 1999], and these are documented and tested in detail for the WRF model in the work by *Davis et al.* [2007].

[16] Several changes were made in WRF from the 2004 to the 2005 season, in particular with the implementation of a moving two-way nested, vortex-tracking grid in 2005. Also, among other things, the frictional velocity was specified to be too small over the ocean in 2004 and 2005, but corrected for the Katrina runs used here [*Davis et al.*, 2007]. When modified to be more realistic, winds generally decreased, as did the minimum central pressure and the size of the eye. The biggest change was on the pressure field and radius of maximum winds. So, in the more recent version, the effective enthalpy coefficient is larger, but with weaker winds, all else being equal.

[17] Hence there is a difference in the treatment of the surface layer in the Ivan 2004 simulation versus the Katrina 2005 simulation, presented below. It is not clear how the fluxes change and it has not been considered worthwhile to rerun the Ivan case with the newer model version. Figure 2 presents the radial profile of the azimuthally averaged tangential and radial winds for the times given below for Ivan and Katrina. The vortex is somewhat tighter for Katrina, but not only has the model changed somewhat, so too have the SSTs and synoptic situation in the atmosphere. Hence it would be dangerous to infer too much regarding the differences in radii of maximum winds between Ivan and Katrina, and changes in the absolute magnitudes of the terms in the water budget with respect to SST. We can definitely say that the relative sizes of the various terms in the water budget are very similar in Ivan and Katrina and that this is a robust result.

[18] Examination of surface latent heat fluxes in several major hurricanes simulated by the WRF model revealed peak, azimuthally averaged fluxes between 800 and 1200 W m^{-2} (27.6 to 41.4 mm d^{-1} or 1.15 to 1.73 mm h^{-1}). These storms were Ivan and Frances from 2004 and Katrina and Rita from 2005. Results for Ivan and Katrina are presented

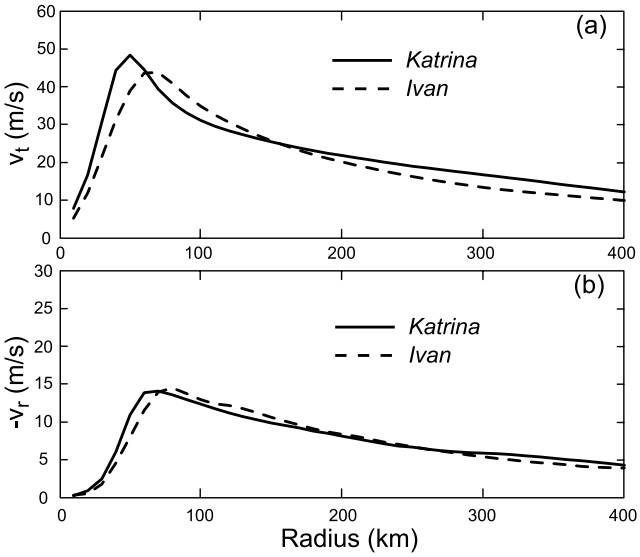

Figure 2. Azimuthally averaged surface (a) tangential and (b) radial winds for simulations of Ivan, 0600 to 1800 UTC 14 September 2004, and Katrina, 1800 UTC 28 August to 0600 UTC 29 August 2005.

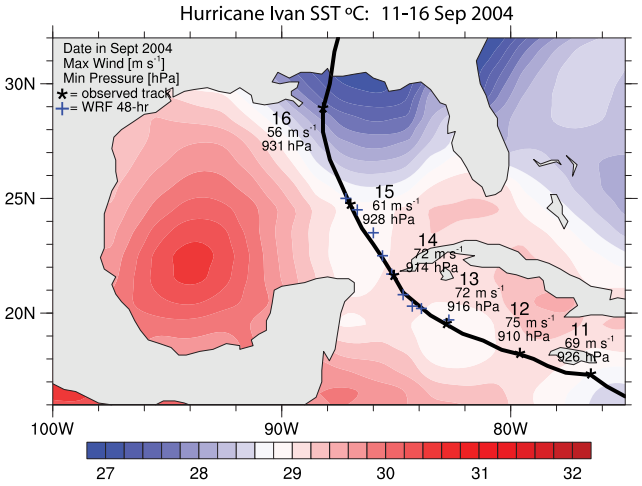

Figure 3. Hurricane Ivan, 11–16 September 2004, along with mean SST for the same period. The observed location (asterisks) on the dates are given along with maximum wind in m s^{-1} and central pressure in hPa. At landfall, Thursday, 16 September, Ivan was a category 3 hurricane, with 130 mph sustained winds and a central pressure of 943 hPa. The WRF forecast track locations every 6 h are given by blue pluses.

in some detail. Peak rainfall rates were generally consistent with the *Lonfat et al.* [2004] climatology, averaging approximately 8–15 mm h^{-1} in the eye wall region (30–70 km radius). Thus even for hurricanes, where the surface evaporation rates in the model are 5 to 10 times the background rates, rainfall amounts are greater by an order of magnitude in the inner part of the storm.

3.1. Ivan

[19] Results for Ivan are now detailed for one particular simulation. Hurricane Ivan occurred in September 2004 and Figure 3 shows the forecast path and actual track of Ivan. The background field of SST for the same interval partly reflects the cold wake left behind Ivan, with SST cooling of 3–7°C in two areas along Ivan's track [*Walker et al.*, 2005]. The lower boundary condition for the model was for SSTs between 29 and 30°C throughout the integration in the neighborhood within 400 km of the eye. To examine the storm, we use a coordinate centered on the eye of the storm, and generate statistics for the azimuthal mean, such as those given in Figures 4 and 5. The wind velocity is detailed in Figure 4 for the tangential and radial components, and the latter is typically much smaller except very locally in the vicinity of the eyewall. The first 12 h are the main time when the storm is spinning up from the coarse resolution input initial state and this time has been excluded from the figures. In the case of Ivan, results computed for the whole storm and ocean-only areas were virtually identical, and only the former are shown.

[20] The moisture budget of the storm, as seen by the precipitation and surface latent heating (or moisture) fluxes (note that 29 W m^{-2} latent heat flux corresponds to an evaporation rate of 1 mm d^{-1}) (Figure 5), allows the large-scale bulk flow of moisture to be diagnosed. Integrating from the center outward to 100 and 400 km radii produces values given in Table 1 in the same units for the moisture variables (mm h^{-1}). For 0600 to 1800 14 September 2004 averages inside R = 100 km and R = 400 km radius, the ratio of precipitation to surface moisture flux is 12.9 and 4.95, respectively. The surface latent heat flux falls off from the eye and, relative to the peak values near 60 km radius, values drop per unit area by a factor of 2 at about 270 km radius. However, even though the drop off is much sharper

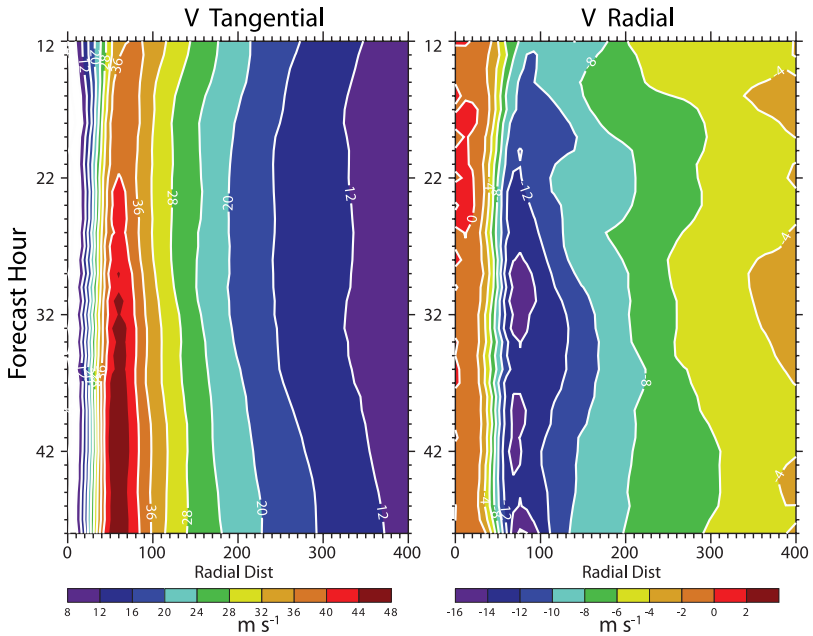

Figure 4. For Hurricane Ivan, given as a function of time after 12 h throughout the 48 forecast starting 0000 UTC 13 September 2004, azimuthal means from the eye of surface wind (left) tangential and (right) radial velocity in m s^{-1}. The hourly values have been smoothed with a 9 point filter.

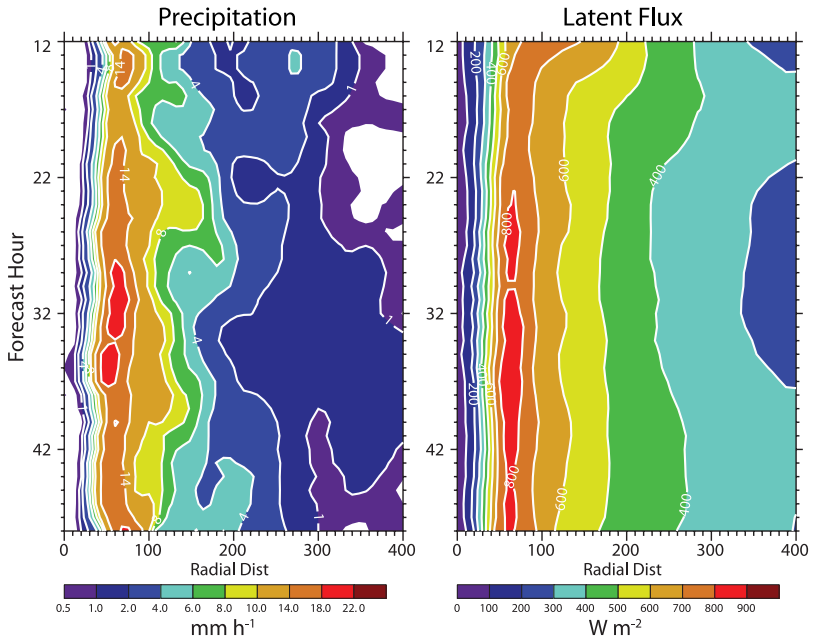

Figure 5. For Hurricane Ivan, given as a function of time throughout the 48 forecast starting 0000 UTC 13 September 2004, azimuthal means from the eye of (left) hourly rain rate, in mm h^{-1}, and (right) surface latent heat flux, in W m^{-2}. Note that 696 W m^{-2} corresponds to 1 mm h^{-1}. The hourly values have been smoothed with a 9 point filter.

for precipitation, it is deduced that one would have to integrate out to about 1600 km radius to obtain a rough balance. *Anthes* [1974] estimated a similar value.

3.2. Katrina With Observed SSTs

[21] For Katrina we consider a 60-h simulation beginning 0000 UTC 27 August 2005 and terminating 1200 UTC 29 August 2005, shortly before it made landfall at 1400 UTC. SSTs under the storm ranged from 303.5 K at 0000 UTC 27 August to 304.2 K at 0000 UTC 29 August, see Figure 6. Changes in SST associated with Katrina's passage [*Davis et al.*, 2007] were in excess of 4°C and just to the right of the storm track. To avoid undue contamination from land, we focus on the period 42 to 54 h into the simulation from 1800 UTC 28 August to 0600 UTC 29 August 2005. Observed maximum winds started at 51 m s^{-1} but rose rapidly, beginning about 0600 UTC 28 August, to 64 m s^{-1}, and peaked at 77 m s^{-1} (category 5) about 1600 UTC 28 August, dropping to 67 m s^{-1} before making landfall just after the end of the run (Figure 6). (Note the maximum wind is not an azimuthal average.) In contrast in the simulated storm (Figure 7), the maximum azimuthally averaged surface

Table 1. Data for the Ivan Simulation Beginning 0000 UTC 13 September 2004 for Hours 30–42 (0600 to 1800 14 September 2004)[a]

	R = 100 km	Units	R = 400 km
Transport	12.4	mm h^{-1}	2.12
Rainfall	13.4	mm h^{-1}	2.97
LH flux	1.04	mm h^{-1}	0.60
V_t	34.9	m s^{-1}	9.91
V_r	−13.0	m s^{-1}	−3.90
SST	302.4	K	302.5

[a]The second and fourth columns are averages inside R = 100 km radius and R = 400 km radius, respectively, and the third column is the units. Given are (1) the vertically integrated transport of moisture into the domain, (2) the rainfall, (3) the surface latent heat flux, (4) the surface tangential velocity V_t, (5) the surface radial velocity V_r, and (6) SST. Note that the mean relative vorticity inside radius R is $2V_t/R$ and the mean divergence is $2V_r/R$. 1 mm/h is 696 W m^{-2}, and over 400 km radius 2.9 mm/h is 1 PW.

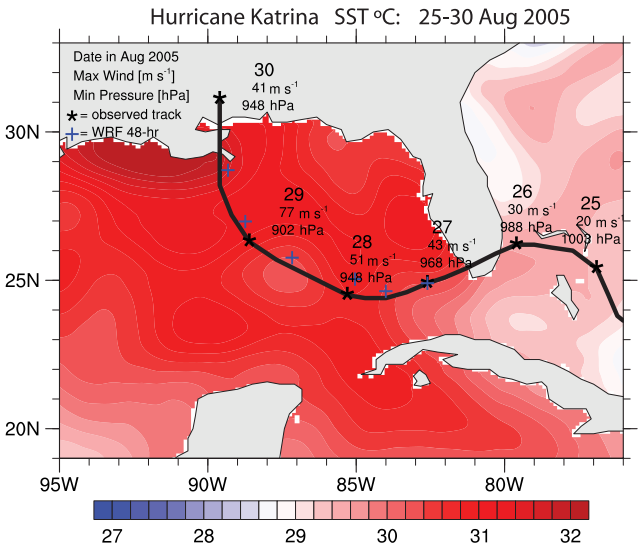

Figure 6. Observed SST, in °C, observed track of Katrina with asterisks to indicate locations on 25 to 30 August (date, top number; maximum wind speed in m s^{-1}, second number; and minimum pressure in hPa, third number) and blue pluses to indicate the WRF simulated location starting 27 August 2005.

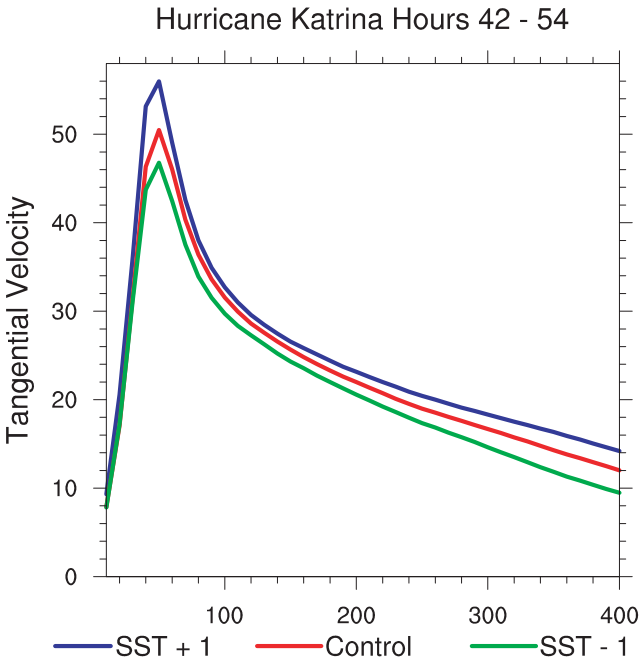

Figure 7. For 1800 UTC 28 August to 0600 UTC 29 August 2005, hours 42 to 54 of the simulation, the azimuthally averaged tangential velocity (m s^{-1}) at the surface as a function of radius for the control (red) and changes in SST of +1°C (blue) and −1°C (green).

winds, which occurred at 38 km radius, gradually increase throughout the simulation and average 51 m s^{-1} from 1800 28 August to 0600 UTC on 29 August. The time sequences of both the azimuthally averaged precipitation and surface latent heat flux show increases along with the winds. As the storm intensifies the radial component of velocity into the storm increases and thus so does low-level convergence of moisture, providing the direct relationship with precipitation, while the latent heat flux depends directly on surface wind speed.

[22] As for Ivan, the ratios of precipitation to surface latent heat (Figure 8) in the various radial bands are large (Table 2): 9.1 inside 100 km radius of the center of the storm and 3.9 integrating out to 400 km radius from the storm center. The surface latent heat flux and the moisture convergence (Figure 8) are comparable at about 700 km radius, and a moisture balance between total surface flux and precipitation is roughly achieved at about 1600 km radius. Table 2 (Figure 8) shows the time-integrated fluxes for surface latent heat, precipitation, and the vertically integrated horizontal flux of moisture. We have also separately computed the moisture convergence below 1 km altitude and, to a first approximation, vertical advection of water vapor is balanced by falling hydrometeors at 1 km altitude. The vertical flux component is very small inside 100 km from the storm center, highlighting the fact that the moisture convergence is mostly from within the lowest 1 km in the boundary layer. However, it is proportionately much larger over the 400 km radius, and comparable to the horizontal convergence. The residuals of the terms are fairly small, but also systematic in sign, and are believed to arise mainly from the temporal sampling in computing the other terms, although artificial moisture sources also play a role, as discussed later.

3.3. Katrina With Changed SSTs

[23] Given the good track forecasts of Katrina, even though the intensity does not vary as observed, experiments have been run whereby the SSTs are changed by +1°C and −1°C uniformly over the domain to help assess how the surface fluxes and moisture transports are affected. As noted earlier, the model vortex starts out weaker than observed and not in equilibrium with the environmental conditions in the control run. Clearly a major part of what happens in the

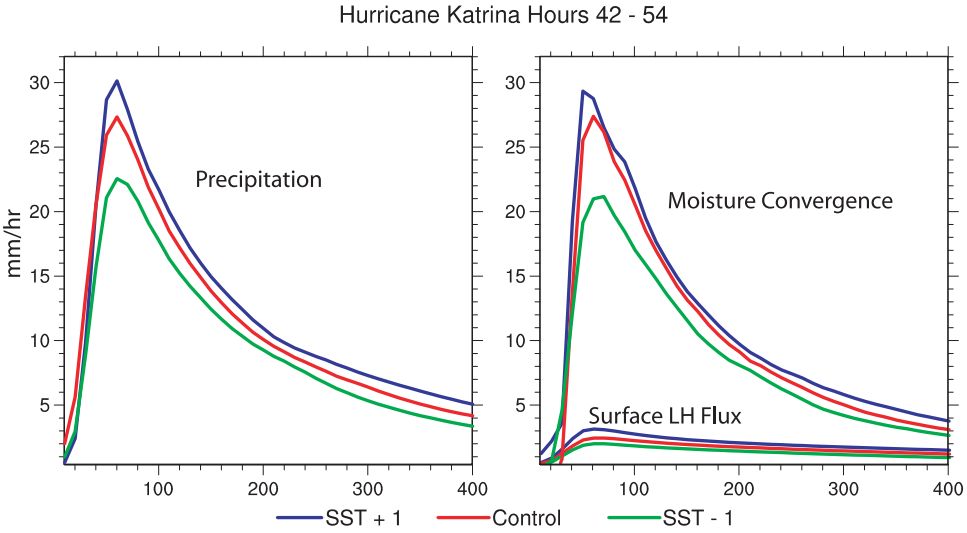

Figure 8. For 1800 UTC 28 August to 0600 UTC 29 August 2005, hours 42 to 54 of the simulation, (left) the azimuthally averaged precipitation (mm h^{-1}) and (right) column integrated moisture convergence and surface latent heat flux as a function of radius for the control (red) and changes in SST of +1°C (blue) and −1°C (green). The precipitation and latent heat fluxes are area averages from the eye to the radius plotted to be compatible with the moisture convergence across that cylinder radius.

Table 2. Data for the Katrina Simulation for Hours 42–54 (1800 UTC 28 August to 0600 UTC 29 August 2005)[a]

	Control R = 100 km	% Change per K SST	Units	Control R = 400 km	% Change per K SST
Wv transport	19.8	11.6	mm h^{-1}	2.68	22.4
Rainfall	19.1	9.4	mm h^{-1}	4.30	18.8
LH flux	2.1	20.2	mm h^{-1}	1.10	25.5
V_t	31.2	4.2	m s^{-1}	12.1	19.0
V_r	−12.4	2.5	m s^{-1}	−4.27	14.9
SST	304.2		K	304.2	
SLP	950.0	−0.78	hPa	982.9	−0.43

[a]For averages inside R = 100 km radius (second and third columns) and averages inside R = 400 km radius (fifth and sixth columns), given are the control value and the percentage change in the variable per K change in SST (normalized by the control), with the units in the fourth column. Measurements include (1) the vertically integrated transport of moisture into the domain, (2) the rainfall, (3) the surface latent heat flux, (4) the tangential velocity, (5) the radial velocity, (6) SST and (7) sea level pressure (SLP). Note that the mean relative vorticity inside radius R is $2V_t/R$ and the mean divergence is $2V_r/R$.

model is an adjustment process and, as surface fluxes change, water vapor in the atmosphere is increased to be more compatible with the SSTs, while radiation responds more slowly. Most of this adjustment occurs within the first day. Nonetheless it is of interest to examine the changes in the hurricane simulation: the intensity (Figure 7), the precipitation, the surface fluxes, and the moisture convergence (Figure 8). The main statistics used are over the 12 h 42 to 54 h into the simulation from 1800 UTC 28 August to 0600 UTC 29 August 2005. This also provides time for equilibration of the storm and the environment to the changed SSTs. In this case there are clear influences of land on the results, and some results are given just for ocean areas.

[24] The evolution of the maximum surface wind and intensity of the vortex is reasonably similar in the three cases, but with the vortex more intense as SSTs increase, as expected from the theory (section 2), see Figure 7. From 28 August 1800 to 29 August 0600 UTC, peak azimuthally averaged surface tangential winds increase with increasing SSTs from 47.0 to 50.5 to 56.0 m s^{-1} or about a change of 4.5 m s^{-1} K^{-1} (about 8.9% of the control). Corresponding minimum sea level pressure, which averaged 920.8 hPa for this period, fell 11.5 hPa K^{-1} increase in SST. Averaged inside a 100 km radius, the tangential winds in the control (31.2 m s^{-1}) increase 4.2% K^{-1} increase in SST (Table 2), but the increase is much larger (19% K^{-1} SST) when the 400 km radius average is considered. The surface pressure fell 7.4 hPa K^{-1} inside 100 km and 4.2 hPa over 400 km radius. Perhaps surprisingly, the surface radial component of the velocity and thus the surface mass convergence into the storm does not appear to change much up to about 270 km from the eye (not shown, but see Table 2). However, the vortex is a bit bigger in the +1°C case, as the inward component strengthened by order 10% between the −1 and +1°C cases at radii of 280 to 400 km and, partly because of increased moisture, the moisture convergence (Table 2) increases substantially. At 100 km radius the moisture convergence goes up 11.6% K^{-1} SST change and at 400 km radius the value is 22.4%.

[25] Precipitation (Figure 8) peaks slightly outside the radius of strongest winds and the increase with increasing SST is 9.4% K^{-1} increase in SST or 1.8 mm h^{-1} averaged inside 100 km radius, but more representative is the fairly uniform increase of 16% of control per K from 50 to 400 km radius, with a net 18.8% increase over the entire 400 km radius. The biggest differences are in the surface latent heat flux (Figure 8) which averages to 25.5% of control per K increase from 0 to 400 km radius, with variations from about 20 to 28%. If we assume that the change is due to only the two terms in the surface flux $V\Delta q$ then an 18.6% increase in wind speed implies a 5.8% increase from the disequilibrium between the atmosphere and ocean in the moisture Δq. This is exactly the change in $q_s(T)$ per K at 30°C from Clausius-Clapeyron. Note that at 30°C, a 1°C increase in temperature with the same specific humidity would reduce the RH from 80% to 75.7% and thus change the $(1-RH)$ factor in (1) by 21%. However, as it is expected that the time to equilibrate is less than a day, this effect is small for 42 to 54 h into the simulation and hence the change can be largely accounted for by the wind speed and saturation specific humidity. Other factors are the eddy terms associated with transients in time and with the asymmetry of the storm and the spiral arm bands, which become more active in higher SSTs, and with some complexity added from land regions where the surface is unchanged.

[26] The increase in moisture convergence (Table 1 and Figure 8) is larger than proposed theoretically in section 2, where it was suggested that the value might be order 14% K^{-1} change in SST. However, that argument was based solely on the average change in atmospheric moisture content and consequential change in vertical motions, and did not account for the change in intensity that has further enhanced the surface latent heat flux, which in turn helps provide the water resource for moisture convergence.

4. Discussion and Conclusions

[27] It is abundantly clear from this and several previous studies that the moisture budget in tropical cyclones is dominated by the inflow of moisture, mainly in the lowest 1 km of the storm. Inside about 100 km of the center of the storm, the moisture inflow is about a factor of 10 greater than the latent heat flux from the surface (12.9 for Ivan and 9.1 for Katrina), in spite of the fact that it is ultimately the latter that mainly causes the inflow to occur. Together these moisture fluxes contribute to the heavy rainfall in tropical cyclones and thus latent heat that drives the storms. The case studies used here have values not much different, perhaps a factor of two larger, than the estimates made in the 1958 storms by *Riehl and Malkus* [1961] and *Miller* [1962], and strengthen several aspects of the *Anthes* [1974] review. Results are also compatible with those for Bonnie [*Braun*, 2006]. For Bonnie the volume-averaged water vapor budget inside 70 km radius had rainfall of 19.6 units

made up of evaporation of 6.8 units, low-level inflow of 16.8 units and outflow at upper levels of 4.6 units (net inflow 12.2 units), where the unit normalization was the total condensation of 1.93×10^{12} kg h^{-1} (equivalent to 1.34 PW). From 70 to 200 km the low-level inflow across 200 km radius was 56.8, the upper troposphere outflow of moisture was 3.2 (net 53.6) and the evaporation was 35.9 while the condensation was 80.4 units. Hence within 200 km radius in Bonnie, 53.6% of the total rain came from moisture convergence and 42.7% came from surface evaporation, with the difference arising from artificial sources.

[28] For Ivan and Katrina inside 400 km radius 71% and 62% of the rainfall, respectively, came from moisture convergence from outside that region. A smaller fraction of the rainfall came from surface moisture fluxes in the case of Ivan, where the SSTs were 1.8°C lower. With lower saturation specific humidity accompanying the lower SSTs, it is expected that the surface flux should be proportionately less. However, there are many variables that come into play. A comparison of the area averages over the 400 km radius domain (Tables 1 and 2) reveals that the Ivan values for the tangential wind are 82% of Katrina's, the precipitation 69%, the surface latent heat flux 55%, and the moisture convergence into the domain 79%. To explain these changes, we note that the saturation specific humidity corresponding to the observed SST change for Ivan is reduced to about 89% of that of Katrina. This, when combined with the wind change, suggests a change in surface latent heat flux to order 73% of the Katrina value, which is not quite as much as found in the model. Changes in the details of the storms, such as size and spiral arm bands discussed later, and model changes account for the differences.

[29] The computed water vapor transport, rainfall and surface evaporative flux do not sum to zero in Tables 1 and 2. For Katrina inside 100 km the transport and evaporation exceed the rainfall somewhat, while over 400 km radius, there is a slight deficit. Although WRF has a much more accurate finite difference scheme than MM5 (used by *Braun* [2006]), it still does not conserve water substance, and infilling negative mixing ratios for water vapor and liquid water should result in a spurious source of moisture, which could be the 8% (Ivan) or 12% (Katrina) excess rainfall found over the 400 km radius, although the moisture budget is also affected by temporal sampling and how it was computed. In particular, largest errors are expected near the eyewall of the storm where liquid water amounts are largest.

[30] Further developments are occurring in the WRF model and these include ocean coupling with a mixed layer ocean model, further increases in resolution, and data assimilation to improve the initial state [*Davis et al.*, 2007]. The resolution is particularly important for details of inner core dynamics, intensity and eyewall structure, while an interactive ocean and improved wave model are vital for improving the surface fluxes and will benefit climate-oriented studies [*Chen et al.*, 2007; *Davis et al.*, 2007].

[31] In our limited experiments, even in a relatively simple setup of uniformly perturbed SST and unchanged boundary conditions, there are some surprising variations of different storm attributes. For instance, (1) the storm expands as SST increases, (2) the inner core intensity varies less than outer circulation, and (3) the inflow maximum was relatively invariant overall, yet the moisture transport increased because of increased "reach" of the storm. This result implies that the key issue regarding hurricane changes with evolving environments may be properties other than the maximum wind speed. In addition, the spiral arm bands become more active in higher SSTs. It will be of interest to see whether these results hold up in further research.

[32] Overall in Katrina simulations the precipitation increased about 19% K^{-1} increase in SST. *Knutson and Tuleya* [2004] find increases in precipitation to be substantial and among the largest changes found when carbon dioxide is increased (roughly doubled) in models, corresponding to SST increases of 0.8 to 2.4°C and averaging 1.75°C (T. Knutson, personal communication, 2006). They find an overall increase of 18% but ranging from 12 to 26% depending on the convective parameterization scheme. In contrast wind speeds increased 6%. However, the increase in atmospheric stability in those models no doubt diminished the size of the increases [*Shen et al.*, 2000]. In our sensitivity tests, we are not trying to emulate the future climate in a greenhouse gas enriched world. How the static stability changes is an outstanding issue because climate models depend on parameterized subgrid-scale convection, and the evidence strongly suggests that models do not do this correctly [*Lin et al.*, 2006], artificially stabilizing the atmosphere at the expense of resolved transient disturbances of all sorts in the tropics. Observations of changes in atmospheric lapse rate reveal no significant changes, although the quality of the observations leaves much to be desired. The relevant observations come from radiosondes (which have suffered major problems, especially in the tropics [e.g., *Randel and Wu*, 2006]) and microwave sounding unit (MSU) satellite observations (that also have uncertain changes), as discussed extensively in the recent Intergovernmental Panel on Climate Change report [*Trenberth et al.*, 2007].

[33] The enhanced latent heating and intensification of the storm do not exhibit a simple relationship in part because the rainfall may occur in the spiral arm bands away from the core. Short-term fluctuations in intensity arise from complex processes such as eyewall replacement [*Houze et al.*, 2007] and are not well understood or predicted [*Emanuel*, 1999, 2000]. Whether or not the intensity of the storm is affected depends on the covariability of the temperature perturbations and the latent heating, and this will depend on the large-scale dynamics of the storm and atmospheric structure. Various other feedbacks also kick in, and many other processes are known to be important, such as the stability changes, changes in sea spray, frictional effects, cold wake effects on SSTs, and so on. So the net effects could easily be greater or smaller than found here.

[34] Observed and potential changes in hurricanes with global warming are discussed in detail by *Trenberth* [2005], *Emanuel* [2005a, 2005b] and *Webster et al.* [2005] who show that intense storms are observed to be increasing and with longer lifetimes, in line with theoretical and modeling expectations, and this is also evident in our preliminary results for energy exchange [*Trenberth and Fasullo*, 2007]. Empirically there is a very strong relationship between intensity and potential destructiveness of such storms with SSTs in the genesis regions in the tropics [*Emanuel*, 2005a,

2005b]. In summarizing understanding of hurricanes and climate *Emanuel* [2003] notes that increases in greenhouse gases in the atmosphere are likely to require a greater turbulent enthalpy flux out of the ocean (largely in the form of greater evaporation), and has found with a simple model that potential maximum winds would increase by approximately 3.5 m s^{-1} for each 1°C increase in tropical SSTs. *Emanuel* [1988] estimated a sensitivity of the central pressure in the eye as being ~6 hPa K^{-1} of SST, but here we find about 11.5 hPa K^{-1}. Our values in the Katrina experiments find increases of peak wind speed of 4.5 m s^{-1} or about 9% K^{-1} change in SST. These values are not directly comparable because the Emanuel values apply to the potential intensities, not the actual. The surface latent heat flux went up 20 to 25% K^{-1} and we find that this can be largely explained as due only to the two terms in the surface flux $V\Delta q$, and the 5.8% increase from the disequilibrium between the atmosphere and ocean in the moisture Δq is the change in $q_s(T)$ per K at 30°C from Clausius-Clapeyron.

[35] Increases in greenhouse gases from human activities are responsible for most of the broad global increase in surface air temperature and SST since about 1970 [*Intergovernmental Panel on Climate Change*, 2001; *Meehl et al.*, 2004], SSTs in the genesis regions for tropical cyclones [*Santer et al.*, 2006] and warming of the ocean and rising sea level [*Lombard et al.*, 2005; *Barnett et al.*, 2005; *Hansen et al.*, 2005]. Variations in SSTs occur from year to year associated with natural variability, such as El Niño. A linear trend fit for 1970 to 2004 for tropical SSTs between 30°N and 30°S is 0.50 ± 0.25°C, which is associated with an estimated 3.9 ± 2.0% increase in total column water vapor over the oceans (based on *Trenberth et al.* [2005]), and is the main source of moisture for storms. Therefore in tropical storms, we argued in section 2 that moisture convergence $v_r q$ may have experienced average enhancements since 1970 of both v_r and q by order 3.9%, so the total increase is about 7.8% (coming from 1.039^2), and this corresponds to the expected increase in rainfall in the storm, with 3.6 to 11.8% as the 95% confidence limits. This simple theory is reasonably borne out by the numerical experiments presented here, although there is obviously much more to individual storms associated with meteorological conditions and the weather situation, and this does not include allowance for any change in intensity of the storms. We have confirmed the changes in moisture and evaporation with SST in our experiments (as also observed more generally by *Lu and Weller* [2007]). However, the changes in radial velocity depend on where the latent heat is realized, and some occurs in the spiral arm bands. Also it depends on changes in static stability [*Shen et al.*, 2000] and thus is less certain. An alternative possibility from potential intensity theory [*Emanuel*, 2005a] is that the velocity components increase about 4% K^{-1} SST change, or about half that given above, although in Table 2, percent changes in the two velocity components differ. Nevertheless, in that case the total increase in moisture convergence to date would be order 2% and the change in storm rainfall is about 6%.

[36] We have demonstrated that the moisture budget of tropical cyclones is dominated by the large-scale convergence of moisture, as is the case for most meteorological phenomena. This creates a potential dependency on the large-scale environment, although it also depends on the lifetime of tropical storms. Many theories rely on steady state assumptions that cannot be true in most cases. Initial developments depend on moisture in the atmosphere, but as the lifetime of the storm is extended beyond a few days, the large-scale environmental dependency becomes greater on the SSTs and on the surface flux of moisture into the atmosphere, although on quite large scales. The SSTs in turn depend on subsurface ocean heat content if they are to recover from storm-induced heat losses. Hence nearby land can have an influence by limiting the moisture availability and the storm will feel some effects of land long before it makes landfall.

[37] We argued theoretically that as the climate changes, not only does the atmospheric environmental moisture increase at about the rate given by Clausius-Clapeyron, signifying a tendency for fairly constant relative humidity, but the surface latent heat flux into such storms is also affected, as found by *Lu and Weller* [2007]. We conclude that the environmental changes related to human influences on climate have very likely changed the odds in favor of heavier rainfalls and here we suggest that this can be quantified to date to be of order 6 to 8% since 1970. It probably also results in more intense storms. The key point is that the value is not negligible, and nor is it large enough to dominate over the natural processes already in place. In the case of Katrina and New Orleans, where rainfalls locally exceeded 12 inches (305 mm), this would mean an enhancement of about 0.75 to 1 inch (19 to 25 mm). Although incremental, such changes can cause thresholds to be exceeded (the straw that breaks the camel's back) and thus it is appropriate to raise the question of whether this increase in rainfall enhanced flooding and contributed to the breach in New Orleans levees?

[38] **Acknowledgments.** This research is partially sponsored by the NOAA CLIVAR program under grant NA17GP1376. The National Center for Atmospheric Research is sponsored by the National Science Foundation.

References

Anthes, R. A. (1974), The dynamics and energetics of mature tropical cyclones, *Rev. Geophys.*, *12*(3), 495–522.

Barnett, T. P., D. W. Pierce, K. M. AchutaRao, P. J. Gleckler, B. D. Santer, J. M. Gregory, and W. M. Washington (2005), Penetration of human-Induced warming into the world's oceans, *Science*, *309*, 284–287.

Bister, M., and K. A. Emanuel (1998), Dissipative heating and hurricane intensity, *Meteorol. Atmos. Phys.*, *50*, 233–240.

Black, P. G., et al. (2007), Air-sea exchange in hurricanes: Synthesis of observations from the Coupled Boundary Layer Air-Sea Transfer Experiment (CBLAST), *Bull. Am. Meteorol. Soc.*, *88*, 357–374.

Braun, S. A. (2006), High-resolution simulation of hurricane Bonnie (1968). Part II: Water budget, *J. Atmos. Sci.*, *63*, 43–64.

Charnock, H. (1955), Wind stress on a water surface, *Q. J. R. Meteorol. Soc.*, *81*, 639–640.

Chen, S. S., J. F. Price, W. Zhao, M. A. Donelan, and E. J. Walsh (2007), The CBLAST-Hurricane Program and the next-generation fully coupled atmosphere-wave-ocean models for hurricane research and prediction, *Bull. Am. Meteorol. Soc.*, *88*, 311–317.

Davis, C., et al. (2007), Prediction of landfalling hurricanes with the Advanced Hurricane WRF model, *Mon. Weather Rev.*, in press.

Eliassen, A. (1951), Slow thermally or frictionally controlled meridional circulation in a circular vortex, *Astrophys. Norv.*, *5*, 18–60.

Emanuel, K. (1988), The maximum intensity of hurricanes, *J. Atmos. Sci.*, *45*, 1143–1155.

Emanuel, K. A. (1999), Thermodynamic control of hurricane intensity, *Nature*, *401*, 665–669.

Emanuel, K. A. (2000), A statistical analysis of tropical cyclone intensity, *Mon. Weather Rev.*, *128*, 1139–1152.

Emanuel, K. A. (2001), The contribution of tropical cyclones to the oceans' meridional heat transport, *J. Geophys. Res.*, *106*, 14,771–14,781.
Emanuel, K. (2003), Tropical cyclones, *Annu. Rev. Earth Planet. Sci.*, *31*, 75–104.
Emanuel, K. (2005a), Increasing destructiveness of tropical cyclones over the past 30 years, *Nature*, *436*, 686–688.
Emanuel, K. (2005b), Emanuel replies, *Nature*, *438*, E13, doi:10.1038/nature04427.
Hansen, J., et al. (2005), Earth's energy imbalance: Confirmation and implications, *Science*, *308*, 1431–1435.
Houze, R. A., Jr., S. S. Chen, B. F. Smull, W.-C. Lee, and M. M. Bell (2007), Hurricane intensity and eyewall replacement, *Science*, *315*, 1235–1239.
Intergovernmental Panel on Climate Change (2001), *Climate Change 2001: The Scientific Basis—Contribution of Working Group 1 to the Third IPCC Scientific Assessment,* edited by J. T. Houghton et al., 881 pp., Cambridge Univ. Press, Cambridge, U. K.
Kiehl, J. T., and K. E. Trenberth (1997), Earth's annual global mean energy budget, *Bull. Am. Meteorol. Soc.*, *78*, 197–208.
Knutson, T. R., and R. E. Tuleya (2004), Impact of CO_2-induced warming on simulated hurricane intensity and precipitation: Sensitivity to the choice of climate model and convective parameterization, *J. Clim.*, *17*, 3477–3495.
Krishnamurti, T. N., S. Pattnaik, L. Stefanova, T. S. V. Vijaya Kumar, B. P. Mackey, and A. J. O'Shay (2005), The hurricane intensity issue, *Mon. Weather Rev.*, *133*, 1886–1912.
Kurihara, Y. (1975), Budget analysis of a tropical cyclone simulated in an axisymmetric numerical model, *J. Atmos. Sci.*, *32*, 25–59.
Lin, J. L., et al. (2006), Tropical intraseasonal variability in 14 IPCC AR4 climate models. Part I: convective signals, *J. Clim.*, *19*, 2665–2690.
Lombard, A., A. Cazenave, P.-Y. LeTraon, and M. Ishii (2005), Contribution of thermal expansion to present-day sea-level change revisited, *Global Planet. Change*, *47*, 1–16.
Lonfat, M., F. D. Marks Jr., and S. S. Chen (2004), Precipitation distribution in tropical cyclones using the Tropical Rainfall Measuring Mission (TRMM) microwave imager: A global perspective, *Mon. Weather Rev.*, *132*, 1645–1660.
Lu, L., and R. A. Weller (2007), Objectively analyzed air-sea heat fluxes for the global ice-free oceans (1981–2005), *Bull. Am. Meteorol. Soc.*, *88*, 527–539.
Malkus, J., and H. Riehl (1960), On the dynamics and energy transformations in steady-state hurricanes, *Tellus*, *12*, 1–20.
Meehl, G. A., W. M. Washington, C. M. Ammann, J. M. Arblaster, T. M. L. Wigley, and C. Tebaldi (2004), Combinations of natural and anthropogenic forcings in twentieth-century climate, *J. Clim.*, *17*, 3721–3727.
Michalakes, J., S. Chen, J. Dudhia, L. Hart, J. Klemp, J. Middlecoff, and W. Skamarock (2001), Developments in teracomputing, in *Proceedings of the Ninth ECMWF Workshop on the Use of High Performance Computing in Meteorology,* edited by W. Zwieflhofer and N. Kreitz, pp. 269–276, World Sci., Singapore.
Miller, B. I. (1962), On the momentum and energy balance of hurricane Helene (1958), *Natl. Hurricane Res. Proj. Rep.* 53, 19 pp., U. S. Weather Bur., U. S. Dep. of Commer., Miami, Fla.
Nieman, P. J., and M. A. Shapiro (1993), The life cycle of an extratropical marine cyclone. Part I. Frontal-cyclone evolution and thermodynamic air-sea interaction, *Mon. Weather Rev.*, *121*, 2153–2176.
Noh, Y., W. G. Cheon, S. Y. Hong, and S. Raasch (2003), Improvement of the K-profile model for the planetary boundary layer using large eddy simulation, *Boundary Layer Meteorol.*, *107*, 401–427.
Palmén, E., and C. W. Newton (1969), *Atmospheric Circulation Systems*, 603 pp., Elsevier, New York.
Palmén, E., and H. Riehl (1957), Budget of angular momentum and energy in tropical cyclones, *J. Meteorol.*, *14*, 150–159.
Randel, W. J., and F. Wu (2006), Biases in stratospheric temperature trends derived from historical radiosonde data, *J. Clim.*, *19*, 2094–2104.
Riehl, H., and J. S. Malkus (1961), Some aspects of hurricane Daisy, 1958, *Tellus*, *13*, 181–213.
Santer, B. D., et al. (2006), Forced and unforced ocean temperature changes in Atlantic and Pacific tropical cyclogenesis regions, *Proc. Natl. Acad. Sci. U.S.A.*, *103*, 13,905–13,910.
Shen, W., R. E. Tuleya, and I. Ginis (2000), A sensitivity study of the thermodynamic environment on GFDL model hurricane intensity: Implications for global warming, *J. Clim.*, *13*, 109–121.
Skamarock, W. C., J. B. Klemp, J. Dudhia, D. O. Gill, D. M. Barker, W. Wang, and J. G. Powers (2005), A description of the advanced research WRF version 2, *NCAR Tech. Note TN-468+STR,* 88 pp., Natl. Cent. for Atmos. Res., Boulder, Colo.
Trenberth, K. E. (1998), Atmospheric moisture residence times and cycling: Implications for rainfall rates with climate change, *Clim. Change*, *39*, 667–694.
Trenberth, K. E. (1999), Atmospheric moisture recycling: Role of advection and local evaporation, *J. Clim.*, *12*, 1368–1381.
Trenberth, K. E. (2005), Uncertainty in hurricanes and global warming, *Science*, *308*, 1753–1754.
Trenberth, K. E., and J. Fasullo (2007), Water and energy budgets of hurricanes and implications for climate change, *J. Geophys. Res.*, doi:10.1029/2006JD008304, in press.
Trenberth, K. E., and C. J. Guillemot (1998), Evaluation of the atmospheric moisture and hydrological cycle in the NCEP/NCAR reanalyses, *Clim. Dyn.*, *14*, 213–231.
Trenberth, K. E., and L. Smith (2005), The mass of the atmosphere: A constraint on global analyses, *J. Clim.*, *18*, 864–875.
Trenberth, K. E., and D. P. Stepaniak (2003a), Co-variability of components of poleward atmospheric energy transports on seasonal and interannual timescales, *J. Clim.*, *16*, 3690–3704.
Trenberth, K. E., and D. P. Stepaniak (2003b), Seamless poleward atmospheric energy transports and implications for the Hadley circulation, *J. Clim.*, *16*, 3705–3721.
Trenberth, K. E., and D. P. Stepaniak (2004), The flow of energy through the Earth's climate system, *Q. J. R. Meteorol. Soc.*, *130*, 2677–2701.
Trenberth, K. E., A. Dai, R. M. Rasmussen, and D. B. Parsons (2003), The changing character of precipitation, *Bull. Am. Meteorol. Soc.*, *84*, 1205–1217.
Trenberth, K. E., J. Fasullo, and L. Smith (2005), Trends and variability in column integrated atmospheric water vapor, *Clim. Dyn.*, *24*, 741–758.
Trenberth, K. E., et al. (2007), Observations: Surface and atmospheric climate change, in *Climate Change 2007: The Physical Science Basis—Contribution of WG 1 to the Fourth Assessment Report of the Intergovernmental Panel on Climate Change*, edited by S. Solomon et al., pp. 235–336, Cambridge Univ. Press, Cambridge, U. K.
Walker, N. D., R. R. Leben, and S. Balasubramanian (2005), Hurricane-forced upwelling and chlorophyll a enhancement within cold-core cyclones in the Gulf of Mexico, *Geophys. Res. Lett.*, *32*, L18610, doi:10.1029/2005GL023716.
Webster, P. J., G. J. Holland, J. A. Curry, and H. R. Chang (2005), Changes in tropical cyclone number, duration and intensity in a warming environment, *Science*, *309*, 1844–1846.

C. A. Davis, J. Fasullo, and K. E. Trenberth, National Center for Atmospheric Research, Boulder, CO 80307, USA. (trenbert@ucar.edu)